

# Rhythmic Constraints on Hippocampal Processing: State and Phase-Related Fluctuations of Synaptic Excitability During Theta and the Slow Oscillation

Kurt P. Schall,<sup>1</sup> Jon Kerber,<sup>1</sup> and Clayton T. Dickson<sup>1,2,3</sup>

<sup>1</sup>Departments of Psychology, <sup>2</sup>Physiology, and <sup>3</sup>Centre for Neuroscience, University of Alberta, Edmonton, Alberta, Canada

Submitted 15 August 2007; accepted in final form 21 November 2007

**Schall KP, Kerber J, Dickson CT.** Rhythmic constraints on hippocampal processing: state and phase-related fluctuations of synaptic excitability during theta and the slow oscillation. *J Neurophysiol* 99: 888–899, 2008. First published November 11, 2007; doi:10.1152/jn.00915.2007. Coordinated patterns of state-dependent synchronized oscillatory activity have been suggested to play differential roles in both the encoding and consolidation phases of hippocampal-dependent memories. Previous studies have concentrated on the mutually exclusive patterns of theta and sharp-wave/ripple activity because these were thought to be the only collective oscillatory patterns expressed in the hippocampus. Recently we (and others) have described a novel rhythmic activity expressed during anesthesia and deep sleep, the hippocampal slow oscillation (SO). In an attempt to describe the differential effects of theta and the SO on processing in the hippocampal circuit, we performed evoked potential analysis of two major pathways (the commissural and perforant) in urethane-anesthetized rats across spontaneously expressed theta and SO states. We show that synaptic excitability was significantly enhanced in all pathways during the SO as compared with theta with the exception of the medial perforant path to the dentate gyrus, which showed greater excitability during theta. Furthermore, within each ongoing rhythm, there was a phase-dependent modulation of synaptic excitability. This occurred across all sites and similarly favored the falling phase (positive to negative) of both theta and the SO. Differential effects on the input, processing, and output circuitries of the hippocampus across mutually exclusive coordinated oscillatory patterns expressed during different states may be relevant for the staging of memory processes in the medial temporal lobe.

## INTRODUCTION

Neural processing in the hippocampus (HPC) is crucial for declarative memory processes (Eichenbaum 2004). One of the major features of the activity in this region is the prevalence of collective oscillatory patterns that are expressed differentially during diverse behaviors and across the various stages of sleep. These synchronized patterns are thought to constrain and modulate hippocampal processing and are also considered as important influences for the expression of synaptic plasticity (Axmacher et al. 2006; Buzsáki 2002; Jensen and Lisman 2005). The two most-studied oscillatory patterns in the HPC are the theta rhythm, which is a large-amplitude, 3- to 12-Hz oscillation that appears during exploratory behavior and during rapid-eye-movement (REM) sleep (Bland 1986; Buzsáki 2002; Vanderwolf 1969; Vanderwolf et al. 1977), and sharp wave/ripple complexes, which are transient and irregularly occurring high-frequency (150–250) oscillations that appear during awake immobility, “involuntary” behaviors, and non-REM

sleep (Buzsáki 1986; Suzuki and Smith 1987). Due to their different behavioral state dependencies, these two patterns are mutually exclusive and are thought to contribute differentially to sequential stages of memory processing (Buzsáki 1989). Interestingly, both patterns can also be spontaneously and alternately exhibited during urethane anesthesia (Ylinen et al. 1995a), which provides a tractable system to explore their influence on neurophysiological processing.

Recently, we have described a novel form of collective hippocampal activity—the slow oscillation (SO) (Wolansky et al. 2006). The SO consists of a large-amplitude slow (~1 Hz) extracellular rhythm that appears during deep slow-wave sleep as well as under urethane anesthesia. This pattern is similar to the SO that has been described in the neocortex (Steriade et al. 1993) and has been similarly demonstrated to correspond to swings of the membrane potential of hippocampal neurons from depolarized (spiking) levels to hyperpolarized (nonspiking) levels (so-called “up” and “down” states, respectively) (Hahn et al. 2006, 2007; Ji and Wilson 2007; Wolansky et al. 2006) cf. (Isomura et al. 2006). The SO is a state with electrographic and single-unit activity characteristics that separate it from either theta or the large-amplitude irregular activity state (LIA: during which sharp-wave/ripple complexes occur).

Interestingly, the hippocampal SO shows a dynamic and transient correlation with the neocortical SO that would allow for the synchronization (or alternatively desynchronization) of hippocampal and neocortical neuronal ensembles (Wolansky et al. 2006). Thus the SO could be a candidate platform for establishing bidirectional synaptic plasticity either via long-term potentiation or depression in an extended cortico-hippocampo-cortical circuit. Importantly in this regard, recent studies have suggested that non-REM sleep (and in particular the SO) is important for the consolidation of declarative (i.e., hippocampal-dependent) forms of memory (Bodizs et al. 2002; Marshall et al. 2006; Rasch et al. 2007). Given that the SO only appears during non-REM sleep, it may be that its pattern of collective brain-wide engagement is central to a systems-level consolidatory process.

To examine the influence of this novel state on the neurophysiological properties of the HPC, we performed evoked-potential analysis of the connections between areas CA3 and CA1 of the HPC (via the commissural or Schaeffer collateral pathway), between layer II cells of the entorhinal cortex and the dentate gyrus (DG) of the HPC [the medial perforant path (MPP) and lateral perforant path (LPP)], and between layer III

Address for reprint requests and other correspondence: C. T. Dickson, Depts. of Psychology and Physiology, and Centre for Neuroscience, University of Alberta, P217 Biological Sciences Bld., Edmonton, Alberta, T6G 2E9, Canada (E-mail: cdickson@ualberta.ca).

The costs of publication of this article were defrayed in part by the payment of page charges. The article must therefore be hereby marked “advertisement” in accordance with 18 U.S.C. Section 1734 solely to indicate this fact.

cells of the entorhinal cortex and area CA1 of the HPC [the temporal ammonic (TA) pathway]. Our results demonstrate that these pathways can exhibit differential modulation dependent on state (i.e., greater excitability during either theta or SO) but that all show a rhythmical modulation of excitability that is dependent on the ongoing phase of the given rhythm.

## METHODS

Data were obtained from 29 male Sprague Dawley rats weighing 166–370 g [ $262.63 \pm 15.06$  (SE) g]. All methods used conformed to the guidelines established by the Canadian Council on Animal Care and the Society for Neuroscience and were approved by the Biosciences Animal Policy and Welfare Committee of the University of Alberta.

### *Surgical, implantation, recording, and stimulating procedures*

Animals were initially induced with gaseous isoflurane mixed with medical O<sub>2</sub> at a minimum alveolar concentration (MAC) of 4 in an enclosed anesthetic chamber. After loss of righting reflexes, they were maintained on isoflurane (2.0–2.5 MAC) via a nose cone and implanted with a jugular catheter. Isoflurane was discontinued, and general anesthesia was achieved using slow intravenous administration of urethan (0.8 g/ml; final dosage,  $1.8 \pm 0.03$  g/kg) via the jugular vein. Body temperature was maintained at 37°C using a servo-driven system connected to a heating pad and rectal probe (TR-100; Fine Science Tools, Vancouver, BC, Canada) for the remainder of the surgical and recording procedures. Level of anesthesia was assessed throughout the experiment by monitoring reflex withdrawal to a hind paw pinch. If any visible withdrawal occurred, the animal was administered a supplemental dose (0.01 ml) of urethan.

When the rats no longer exhibited a withdrawal reflex, they were moved to a stereotaxic apparatus for electrode placement. Stereotaxic coordinates were calculated from bregma and respective holes were drilled in the skull to allow electrode penetration in the brain. For single-electrode recordings, a single microwire (Teflon-coated stainless steel wire with a bare diameter of 125  $\mu$ m; A-M Systems, Carlsborg, WA) was implanted at the level of stratum radiatum of area CA1 (AP, -3.3; ML,  $\pm 1.8$  to  $\pm 2.1$ ; DV, -2.5 to -3.2) or the molecular layer of the DG (AP, -3.3; ML,  $\pm 1.8$  to  $\pm 2.1$ ; DV, -2.7 to 3.5). These placements were optimized for commissural and perforant path (PP) stimulation, respectively (see further in the following text). In some cases, a 16-contact linear multiprobe (100- $\mu$ m spacing; Neuronexus Technologies, Ann Arbor, MI), was implanted in the vertical plane using the same coordinates as described in the preceding text for single electrodes. The depth was optimized for recording responses to either or both CA3 or PP stimulation.

For recordings from CA1, evoked potentials (EPs) were elicited by stimulating the contralateral CA3 area using an implanted bipolar electrode constructed from two twisted Teflon-insulated stainless steel wires (110  $\mu$ m bare diameter) at the following coordinates (AP, -3.5; ML, -3.5; DV, -3.0 to -4.0). DG responses were recorded by stimulation of the ipsilateral PP (AP, -7.0; ML, -4.0 to -5.5; DV, -1.5 to -2.5) using an identical electrode. After the recording electrode was lowered into the general area (either CA1 or DG), the stimulating electrode was lowered until a negative-going EP was elicited by stimulating with a 0.2-ms biphasic current pulse at an intensity range of 30–210  $\mu$ A, using an isolated constant current pulse generator (Model 2100; A-M Systems). Both electrodes were then adjusted to ensure a maximal response.

Single-electrode (monopolar) recordings were referenced to ground (stereotaxic apparatus) and amplified at a gain of 1,000 and filtered between 0.1 and 500 Hz using a differential AC amplifier (Model 1700; A-M Systems). Signals from the probe were also referenced to

ground and amplified at a final gain of 1,000 and wide-band filtered between 0.7 Hz and 10 kHz via a 16-channel head stage (unity gain) and amplifier system (Plexon, Dallas, TX). All signals were digitized with a Digidata 1322A A-D board connected to a Pentium PC running the AxoScope acquisition program (Molecular Devices; Union City, CA). Signals were sampled at  $\geq 1$  kHz and were digitized on-line after being low-pass filtered at 500 Hz (software controlled).

### *Experimental procedure*

After suitable sites were located, an input/output curve was constructed by recording the response evoked at increasing levels of intensity of stimulation. In this way, both threshold and maximal values of current injection could be assessed. Subsequently, EPs were elicited at a stimulus intensity that evoked a population excitatory postsynaptic potential (pEPSP, also referred to as a field EPSP) at 70% of the maximum response. It was ensured that for experiments involving slope measurements of the pEPSP component of the EP that the current intensity used did not produce a population spike. The interstimulus interval was  $\geq 8$  s. In all experiments, an average EP or EP profile was recorded using a minimum of 16 sweeps. In experiments where the effects of stimulation of the PP were assessed using the multiprobe, an average paired-pulse profile (using an interpulse interval of 50 ms) was also recorded. Continuous recordings of spontaneous electroencephalographic (EEG; i.e., hippocampal local field potential) activity were also made over a 10- to 20-min period and ensured that alternations between activated (theta) and deactivated (SO) states were spontaneously occurring in the HPC (Wolansky et al. 2006). After recording of these spontaneous records, EPs were collected every 10 s across both spontaneous theta and slow oscillation states. Sweeps were 8 s in length, which was long enough to allow a positive determination of state based on spectral and autocorrelation analysis of sweeps. In addition, it allowed for a determination of the phase of the spontaneous cycle at the point of stimulation (2–3 s into the sweep).

After recording sessions, a small lesion was made at the tip of all single recording and stimulating electrodes by passing 1 mA of DC current for 5 s using an isolated constant current pulse generator (Model 2100; A-M Systems). To make the multiprobe track visible for histological purposes, the probe was moved slightly in two horizontal planes at its most ventral position.

### *Histological procedure*

Rats were perfused transcardially, initially with physiological saline then with 4% Para formaldehyde in saline. Brains were extracted and stored overnight in 30% sucrose in 4% Para formaldehyde. The tissue was frozen with compressed CO<sub>2</sub> and sliced at 60  $\mu$ m with a rotary microtome (1320 Microtome; Leica, Vienna). Slices were then mounted on gel-coated slides, allowed to dry for a minimum of 24 h, subsequently stained using thionin, and fitted with a coverslip. Microscopic inspection of stained slices was used to verify recording loci. Digital photomicrographs (Canon Powershot S45; Canon, Tokyo, Japan) were taken on a Leica DM LB2 microscope, imported using Canon Remote Capture 2.7 software and processed with Corel PhotoPaint (Corel, Ottawa, Ontario, Canada).

### *Data analysis*

**POPULATION EPSP SLOPE AND STATE MEASUREMENTS.** The slope of the population pEPSP response was assessed by fitting a line to the initial negative component of the EP (Clampfit version 9.0 Molecular Devices). Slopes were computed for individual trace and were then averaged and compared as a function of EEG state and the phase of the ongoing spontaneous oscillation cycle. Slope measurements of the pEPSP component were chosen over measures of amplitude because the former correlate directly with the strength of synaptic transmission

and are less subject to spurious field artifacts (Johnston and Wu 1995, p. 432–435). EEG state was classified as theta or SO based on the power spectrum and autocorrelation computed for each trace (Wolansky et al. 2006). Threshold power values for each of the SO (0.5–1.5 Hz) and theta (3–4 Hz) bandwidths were computed from the temporal variation of power values within these bandwidths derived from spontaneous EEG collected prior to stimulation trials. Traces that had suprathreshold power values for the SO and subthreshold power values for theta bandwidths were designated as SO, whereas conversely traces with suprathreshold power values for theta and subthreshold power values for SO bandwidths were designated as theta. Confirmation of a rhythmic state was achieved by subsequent assessment of rhythmicity in the autocorrelation function (Wolansky et al. 2006). Traces without rhythmicity were classified as LIA.

**OSCILLATORY PHASE DETERMINATION.** For confirmed rhythmic states (either theta or the SO), the phase value at which the EP was triggered was calculated by fitting a sine wave to the bandwidth filtered EEG (3–4 Hz for theta and 0.5–1.5 Hz for SO). Phase was computed relative to the upward zero crossings of the oscillatory signal directly before and after the EP as a function of the period of the full sine wave connecting these two zero crossings. These values were then translated to a degree scale (from 0 to 360) where 0 signified the initial upward zero crossing, 90 the positive peak, 180 the downward zero crossing, 270 the negative peak, and 360 the final upward zero crossing of the sine function. Slope values of the pEPSP were measured as above for individual EPs. To eliminate any contamination of the ongoing rhythm to these slope measurements, we also computed slope values of the field activity just prior (50 ms) to the stimulation and subtracted these values from the pEPSP slope measurements (Wyble et al. 2000). Averaged slope values across phase windows were normalized to both their minimum and maximal values within each experiment to compute summary statistics.

**CURRENT SOURCE DENSITY.** Current source density (CSD) analysis was conducted on spontaneous and averaged field potential profiles recorded using the linear multiprobe following the assumptions of Freeman (1975), Ketchum and Haberly (1993), and Rodriguez and Haberly (1989). An advantage of this form of analysis is that it is completely immune to volume-conducted potentials because it provides an estimate of transmembrane current flow (Johnston and Wu 1995, p. 435–438). Briefly, CSD was computed by estimating the second spatial derivative of unfiltered voltage traces derived from the multiprobe. This estimate was calculated using a three-point difference (differentiation grid size of 300  $\mu\text{m}$ ) on the voltage values across spatially adjacent traces

$$\text{CSD} = [f(p_{i-1}) - 2f(p_i) + f(p_{i+1})]/d^2 \quad (1)$$

Where  $f(p_i)$  is the field signal from probe channel  $i$  ( $i = 2, 3, \dots, 14$ ) and  $d$  is the distance between adjacent channels (0.1 mm).

**DATA SUMMARY AND STATISTICS.** Arithmetic averages were computed within and between experiments and were reported together with the SE. Comparisons of interest were conducted using one-tailed paired  $t$ -test using an alpha (probability) value of 0.05. Descriptive circular statistics using the method of Batschelet (as described by Zar 1999, p. 608–610) were used to compute the oscillatory phase angle at which pEPSPs were preferentially maximal on binned slope data (bin width: 18°). Normalized slope values were used as vector lengths for each of the center points of the phase angle windows. These analyses were conducted on both individual experiments and the average across all experiments. The distribution of the preferred phases across all individual experiments was tested for homogeneity using the method of Hotelling (as described by Zar 1999, p. 638–639).

## RESULTS

### *Histological findings*

We confirmed the location of all single-electrode and multiprobe locations. All CA1 recording positions were in the mid-apical dendritic layer of CA1 pyramidal cells (centered at s. radiatum or at the border with s. lacunosum moleculare). All DG recording positions were at the level of the hippocampal fissure or lower (in the molecular layer of the DG). Stimulation sites in the contralateral CA region were in or near CA3. These sites could be close to the lower blade of the CA3 pyramidal layer, in the mid-apical dendritic zone of s. radiatum of CA3 at the level of its vertical curvature, or in s. radiatum close to the CA1/CA3 border. Stimulation sites aimed at the PP were found to be in or just superior to the dorsal element of the angular bundle. Multiprobe tracts were all in a plane that traversed the CA1 pyramidal cell layer, through the hippocampal fissure and the DG. The termination of probe tracts was typically in s. granulosum or in the hilar region of the DG just ventral to the granule cell layer. The position of individual contact sites was estimated from the position of the histological tract in combination with comparisons to the distribution of spontaneous (theta and SO) and evoked potential profile measures (Wolansky et al. 2006). Summary placements and tracks for all experiments are shown in Fig. 1.

### *State alternations*

As previously described (Wolansky et al. 2006), the activity of the HPC spontaneously alternated between activated (theta), transition (large-amplitude irregular activity: LIA), and deactivated (SO) patterns. All EPs were elicited during and across these spontaneous patterns. By performing spectrographic and autocorrelation analysis of ongoing EEG (Wolansky et al. 2006) for each stimulation trial, we were able to differentiate between all three states. Typical examples of hippocampal theta and SO states are shown in Fig. 2. As demonstrated, theta was characterized by highly rhythmic oscillations in the frequency bandwidth of 3–5 Hz, whereas the SO was characterized by even-larger-amplitude rhythmic oscillations in the 0.5- to 1.0-Hz frequency bandwidth. In comparison, LIA showed a lack of rhythmicity with high power levels across a wider range of the spectrum without clear frequency peaks.

### *Influence of state on EPs*

**CA3-CA1 EPs.** EPs elicited by stimulation of contralateral CA3 and recorded at the level of s. radiatum in CA1 were similar to pEPSPs as previously described (Wyble et al. 2000). They exhibited a maximum negative peak at a latency of  $13.07 \pm 1.61$  ms poststimulation. A typical evoked potential is shown in Fig. 3. Spontaneous alternations among theta, LIA, and SO states resulted in significant variations of synaptic excitability as measured by changes in the slope of the pEPSP. Slope values were consistently (5 of 5) and significantly ( $t = 5.66$ ,  $P = 0.0024$ ) larger during periods of SO as compared with periods of theta. Slope values measured during LIA were intermediate but significantly different to those measured during theta ( $t = 4.63$ ,  $P = 0.0049$ ) and the SO ( $t = 5.19$ ,  $P = 0.0033$ ; Fig. 4).

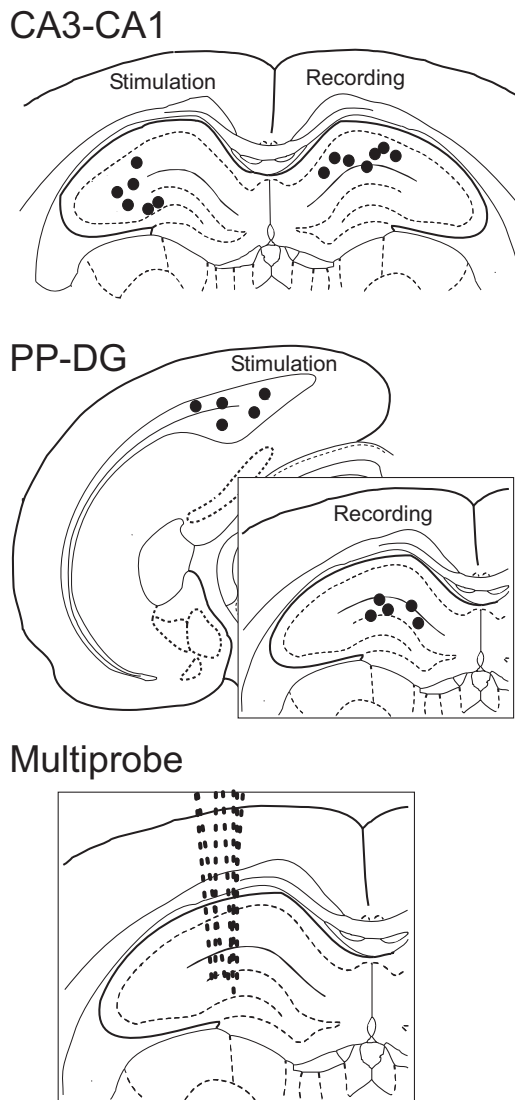


FIG. 1. Summary of histological placements. ●, placements of recording and stimulating electrodes for CA3–CA1 (*top*), perforant path (PP)–dentate gyrus (DG; *middle*), and multiprobe recordings (*bottom*).

Multiprobe recordings through the CA1 region and centered at the level of *s. radiatum* were conducted to further explore the voltage and CSD profiles of CA3 stimulation-evoked EPs. As previously described, the most prominent sink was observed at the level of *s. radiatum*, which also corresponded to the time point of maximal negativity of the evoked potential in this region ( $12.09 \pm 0.49$  ms—see Fig. 5). More importantly, however, the magnitude of this sink was consistently larger during the SO than during theta in this, and all other experiments, and was significantly larger during the SO overall [SO:  $102.61 \pm 32.23$ ; TH:  $88.01 \pm 26.65$ ;  $t(4) = 3.96$ ,  $P = 0.008$ ;  $n = 5$ ; Fig. 5].

PP-DG EPs. EPs elicited by stimulation of the PP and recorded at the level of *s. molecular* in the DG exhibited a maximum negative peak occurring 3- to 8-ms poststimulation. This EP was consistent with pEPSP responses previously described in this region (Canning and Leung 1997; Canning et al. 2000; Leung et al. 1995). Assessment of the variation of synaptic excitability across states through measurement of pEPSP

slopes produced mixed results. Comparing theta to SO, three of five experiments had significantly larger slope values in SO, whereas the other two had significantly larger slope values during theta. In all cases, slope values during LIA were intermediate to those found during theta and SO. In the three experiments in which slopes were largest during the SO, those evoked during LIA were significantly different from both SO and theta in one, and significantly different from SO (but not theta) in the remaining two (Fig. 6). In the two experiments in which slopes were largest in theta, those evoked during LIA were significantly different from theta (but not SO) in one and from SO (but not theta) in the other.

During these initial experiments, we did not differentiate among the various components of the PP (MPP vs. LPP vs. TA). To determine if these different input pathways from the EC to the HPC demonstrated different levels of modulation according to state, we attempted to separate them by mapping their different spatiotemporal properties using simultaneous profile recordings and by assessing their responsiveness to paired pulse stimulation at short latencies. Because the medial, lateral, and temporal ammonic branches of the PP have different laminar terminations zones (MPP: middle third of the DG molecular layer; LPP: outer third of the DG molecular layer; TA: *s. lacunosum molecular* of CA1) and the shape and latency of activation of each of these components are slightly different (MPP < LPP < TA) (Abraham and McNaughton 1984; Canning and Leung 1997; Canning et al. 2000; Leung et al. 1995; McNaughton 1980), the EPs evoked by each of these pathways could be separated. As well, at paired-pulse intervals of 50 ms, the MPP demonstrates depression while the LPP and the TA pathway demonstrate facilitation (Leung et al. 1995; McNaughton 1980). In this way, we were able to determine the identity of the primary pathway (if any) that was activated.

Using these criteria we were able to separate MPP, LPP, and TA components of the EPs even in single experiments as shown in Figs. 7 and 8. In accordance with previous findings (Abraham and McNaughton 1984; Canning and Leung 1997; Canning et al. 2000; Leung et al. 1995; McNaughton 1980), MPP pEPSPs had shorter peak latencies ( $4.12 \pm 0.20$  ms) than LPP pEPSPs ( $5.48 \pm 0.14$  ms) while pEPSPs generated by TA stimulation showed the longest peak latencies ( $6.50 \pm 0.21$  ms). As well, at 50-ms intervals, paired-pulse potentials evoked by MPP stimulation showed depression (on average:  $12.5 \pm 3.1\%$ ) while both LPP and TA EPs were facilitated (on average:  $11.4 \pm 1.4$  and  $17.2 \pm 2.1\%$ , respectively).

More importantly, pEPSPs evoked by stimulation of the MPP as opposed to the LPP and the TA showed opposing relationships with respect to state. The pEPSP slopes of MPP EPs were smaller during SO as compared with theta in four of five experiments and showed a trend to be smaller overall. In general, values during LIA were intermediate, and although they were only significantly different from values during theta in one experiment, they were significantly larger than values during SO in three of the five experiments (Fig. 7A).

In contrast, the slopes of LPP pEPSPs were consistently larger during SO as compared with theta in all ( $n = 5$ ) experiments and were significantly greater overall [ $t(4) = 3.15$ ,  $P = 0.017$ ; Fig. 7]. On average, slope values during LIA were not significantly different to those during theta overall, although in most experiments (4 of 5), they were intermediate between theta and SO values (Fig. 7). However, values during

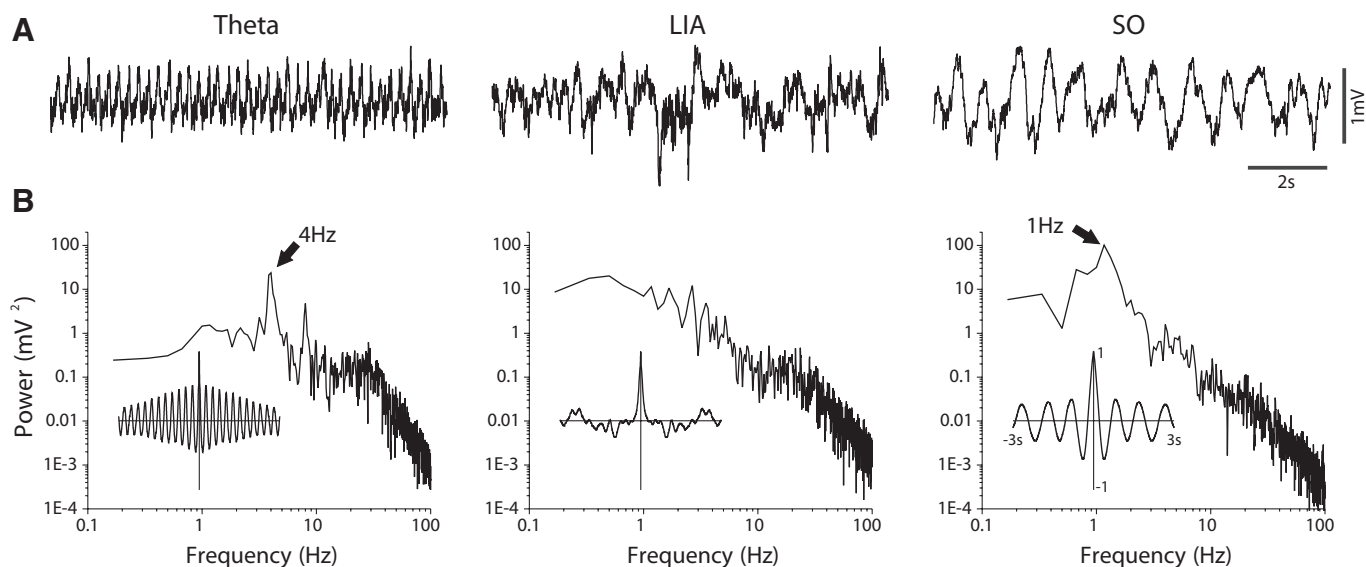


FIG. 2. State-dependent activity of the hippocampus under urethan anesthesia. Spontaneous hippocampal field activity can be classified into 3 states: theta, large-amplitude irregular activity (LIA), or the slow oscillation (SO). Raw traces for each of the 3 states are shown in *A* with their corresponding power spectra and autocorrelations (*insets*) in *B*. Each state can be differentiated based on the raw signal as well as their respective power spectrums and autocorrelations. Theta and the SO are characterized by their rhythmic patterns in the 3- to 4- and 1-Hz bandwidths, respectively, whereas LIA is characterized by a broad bandwidth nonrhythmic pattern.

LIA were significantly lower overall as compared with those measured during SO [ $t(4) = 2.28$ ,  $P = 0.0042$ ].

Similarly to results for the LPP, the slope of TA pEPSPs were consistently larger during SO as compared with theta in all ( $n = 6$ ) experiments (Fig. 7) and were significantly greater overall [ $t(5) = 3.03$ ,  $P = 0.014$ ]. On average, slope values during LIA were intermediate between theta and SO (Fig. 7), and although they were significantly different from those during SO [ $t(5) = 3.08$ ,  $P = 0.0014$ ], they were not significantly different from those during theta.

Further support of this differentiation was obtained in experiments where we conducted multiprobe recordings through CA1 and the DG (Fig. 8). These experiments allowed us to explore the voltage and CSD profiles of PP stimulation-evoked EPs. In some cases (and as shown in Fig. 8), we were able to distinguish all pathways simultaneously. As previously described (Canning et al. 2000), different sinks could be separated based on their spatiotemporal profile corresponding to MPP, LPP, and TA (see preceding text and Fig. 8). Confirma-

tion of different pathways was provided by conducting paired-pulse stimulation and with a combination of histological and profile analysis of spontaneous rhythms (Wolansky et al. 2006). The average magnitude of sinks at these different levels across states were consistent with the slope results for each pathway. For the MPP, sinks were consistently (5 of 5 experiments) and significantly [ $t(4) = 2.54$ ,  $P = 0.032$ ] lower in amplitude during the SO as compared with theta. For the LPP and TA, sinks were consistently (4 of 5 and 4 of 4 experiments, respectively) and significantly larger in amplitude during the SO as compared with theta [LPP:  $t(4) = 2.28$ ,  $P = 0.043$ ; TA:  $t(3) = 3.95$ ,  $P = 0.014$ ; Fig. 8].

#### Influence of oscillatory phase on evoked EPs

In many of our experiments, we noted that there was substantial variation of slope values within each of the oscillatory field states of theta and SO. Previous studies have shown that synaptic excitability as measured by the slope of the pEPSP is

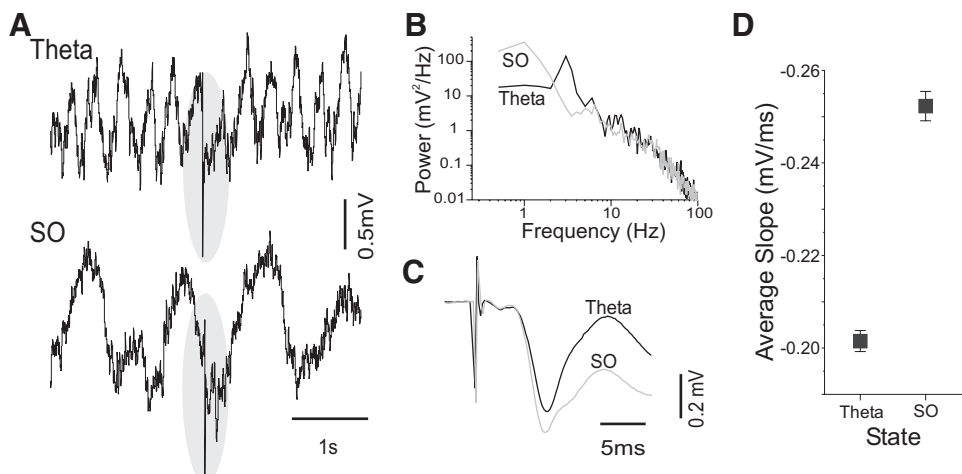
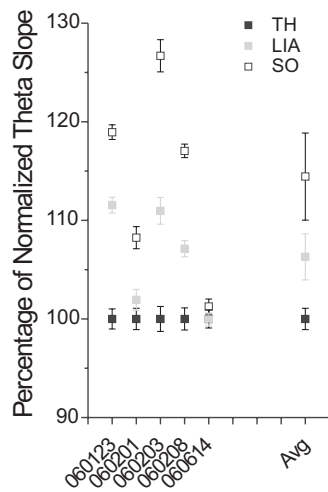


FIG. 3. Influence of state on evoked potentials. *A*: evoked potentials (EPs; highlighted by gray shading) were elicited during ongoing theta (*top*) and the SO (*bottom*) in CA1 via contralateral CA3 stimulation. *B*: power spectra of the spontaneous field potentials confirmed the difference between ongoing states and *C*) average expanded and superimposed sweeps of the EPs across the 2 states demonstrates a larger EP during the SO as compared with theta. *D*: average values of the population excitatory postsynaptic potential (pEPSP) slopes show a significant difference between states with negative slope values higher during the SO.

## CA3-CA1



## PP-DG

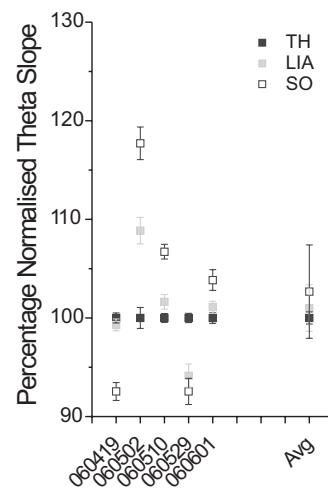


FIG. 4. Influence of state on CA3–CA1 EPs. Average pEPSP slopes evoked during theta (■), LIA (□), and SO (□) are plotted as a normalized percentage of the average amplitude during theta. The pEPSP slopes evoked by CA3 stimulation were consistently and significantly higher during the SO and intermediate during LIA for each experiment and for the overall average across experiments.

FIG. 6. Influence of state on PP-DG EPs. Average pEPSP slopes evoked during theta (■), LIA (□), and SO (□) are plotted as a normalized percentage of the average amplitude during theta. The pEPSP slopes evoked by PP stimulation produced mixed results when compared across states. In 2 experiments, the EPSP slopes were significantly lower, whereas in the other 3, they were significantly higher during the SO. Slopes during LIA tended to be intermediate.

related to the phase of the ongoing theta rhythm and is an important factor in the development of LTP (Greenstein et al. 1988; Hyman et al. 2003; Pavlides et al. 1988; Wyble et al. 2000). We were interested in determining whether the phase of the ongoing SO rhythm in the HPC could also modulate

excitability in a similar way. Therefore we tested the influence of phase of both rhythms on the slope of evoked pEPSPs at all sites. A typical experimental protocol is shown in Fig. 9 using CA1 responses to CA3 stimulation during theta as an example.

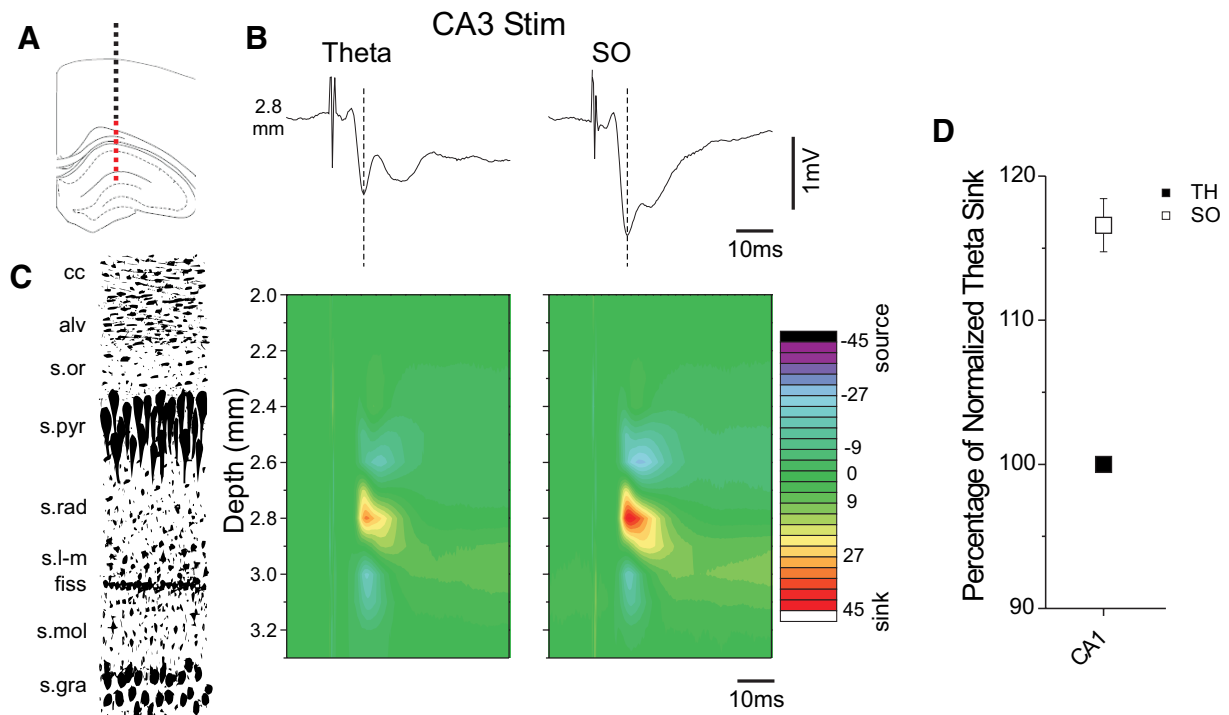


FIG. 5. Comparison of current source density (CSD) in CA1 evoked by CA3 stimulation as a function of state. A 16-contact linear multiprobe was lowered into the hippocampus (HPC) as shown in the diagram in A. B: average evoked potentials from the individual contact showing the largest field negativity after CA3 stimulation (2.8 mm depth – corresponding to stratum radiatum) are shown across both theta and the SO states. Dotted vertical lines denote the time point of maximum negativity in both examples and demonstrate the obvious increase in amplitude during the SO with respect to theta. C: CSD plots of the averaged evoked potential profile showed a larger amplitude sink at the level of s. radiatum (see laminar diagram to right of plots) during the SO as compared with theta. D: normalized averages of sink amplitudes across all ( $n = 5$ ) experiments. On average, the current sinks evoked at the level of s. radiatum during the SO were larger than during theta.

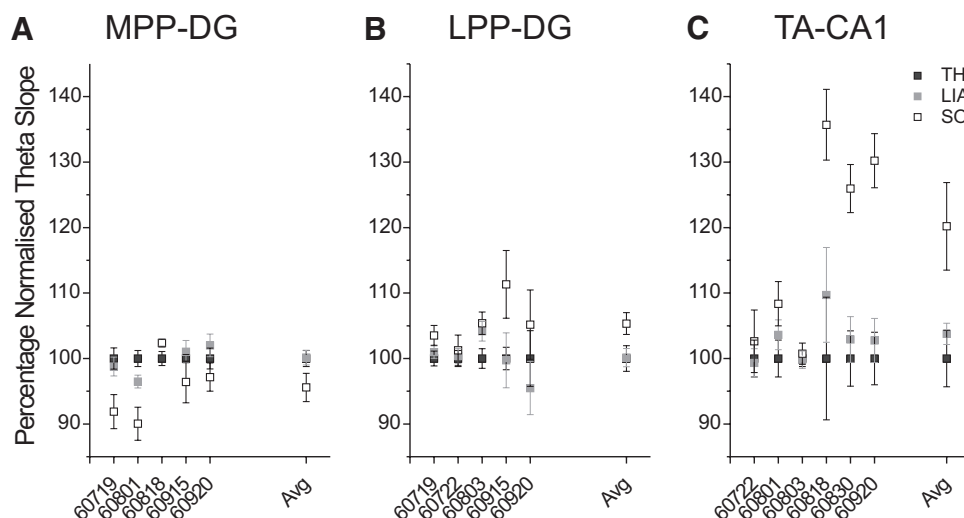


FIG. 7. Comparison of EPSP amplitude (slope) in DG evoked by stimulation of different components of the PP across theta and the SO states. Average EPSP slopes evoked during theta (■), LIA (■), and SO (□) expressed as a normalized percentage of the average amplitude during theta are plotted. *A*: stimulation of the medial PP (MPP) elicited a smaller pEPSP slope during the SO as compared with theta in 4 of 5 experiments, and this difference was significant on average. No significant difference was observed between the average slopes across theta and LIA. *B*: stimulation of the lateral PP (LPP) elicited a larger pEPSP slope during the SO as compared with theta in all experiments, and this difference was significant on average. No significant difference was observed between the average slopes across theta and LIA. *C*: stimulation of the temporal ammonic pathway (TA) elicited a larger pEPSP slope during the SO as compared with theta in all experiments, and this difference was significant on average. Although slopes during LIA were consistently intermediate between theta and SO values, there was no significant difference on average between pEPSP slopes across theta and LIA.

In support of previous findings exhibiting phase influences on synaptic activity during theta (Holscher et al. 1997; Hyman et al. 2003; Rudell and Fox 1984; Rudell et al. 1980; Wyble et al. 2000) and as shown in Fig. 9, we found that the phase of the theta cycle had an obvious influence on the size and slope

of pEPSPs. By separating evoked potentials based on whether they occurred on the rising or falling phases of the theta rhythm, we were able to demonstrate a significant difference in the average slope values. As shown for the example in Fig. 9, the size and slope of the pEPSP was larger during the falling

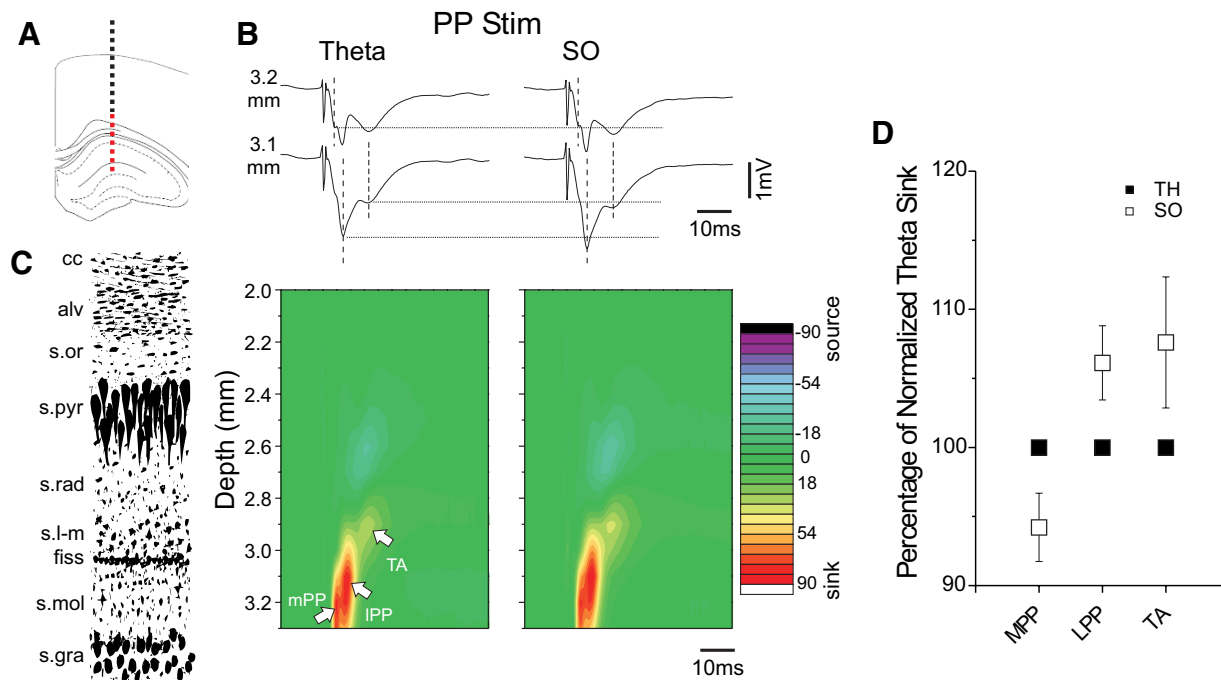


FIG. 8. Comparison of CSD in DG evoked by PP stimulation as a function of state. Data shown come from the same experiment illustrated in Fig. 5. *A*: A 16-contact linear multiprobe was lowered into the HPC as shown in the diagram in *A*. *B*: average evoked potentials from 2 separate contacts showing the largest field negativities corresponding to each respective pathway evoked by PP stimulation (3.2- and 3.1-mm depths) are shown across both theta and the SO states. Dotted vertical lines highlight the respective components: MPP, LPP, and TA in temporal order. Horizontal lines allow a comparison of the relative amplitudes of these components across states. Both LPP and TA showed increases during the SO, whereas the MPP response was lower. *C*: CSD plots of the averaged evoked potential profile show a spatiotemporal dispersion of the sinks corresponding to the 3 components that are highlighted by labeled arrows. Sinks were larger for both the LPP and TA components and smaller for the MPP during the SO. *D*: normalized averages of sink amplitudes across all experiments. On average, the current sinks corresponding to MPP stimulation were smaller, whereas those corresponding to either LPP or TA stimulation were higher during the SO.

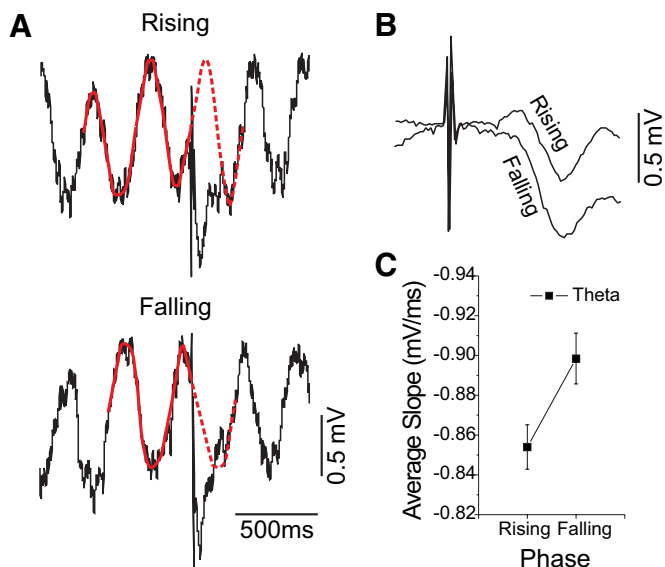


FIG. 9. Phase-dependent modulation of excitability within ongoing oscillatory cycles. *A*: examples of EPs in CA1 evoked by CA3 stimulation induced on the rising (*top*) and falling (*bottom*) phase of the ongoing theta cycle. The calculation of phase was estimated as illustrated by comparison to an idealized sinusoidal like function as illustrated by the overlays in red. *B*: raw EPs for the traces shown in *A* are superimposed at a faster sweep speed for comparison. The EP elicited on the falling phase of the theta cycle is substantially larger. *C*: across all EPs evoked during theta in this experiment, the average pEPSP slope occurring on the falling phase was larger than the average pEPSP slope occurring on the rising phase.

phase and the average difference across multiple trials in the same experiment was significant [ $t(50) = 2.62$ ,  $P = 0.009$ ].

A similar analysis was conducted for both theta and the SO across all experiments. The average results for CA1 and DG EPs are shown in the *left-most panels* in Fig. 10 (*Ai* and *Bi*, respectively). In all cases, there was a significant and similar effect on pEPSP slopes when comparing the rising versus the falling phases of ongoing oscillatory activity. We found no differences in the DG responsiveness to stimulation of the different branches of the PP and thus these data were pooled. Slope values were always significantly larger during the falling as opposed to the rising phase [CA3–CA1 theta:  $t(3) = 4.84$ ,  $P < 0.001$ ; CA3–CA1 SO:  $t(4) = 3.17$ ,  $P = 0.011$ ; PP-DG theta:  $t(5) = 5.65$ ,  $P < 0.001$ ; PP-DG SO:  $t(5) = 5.65$ ,  $P < 0.001$ ].

To more carefully characterize this phase-dependent effect, we arranged stimulation trials in 20 equally sized bins ( $18^\circ$  wide) across the entire cycle and assessed the average normalized pEPSP slope as a function of the phase window in which they occurred. The oscillatory phase angle at which pEPSP slope was preferentially maximal was computed for each experiment and these results are plotted in the *middle panels* of Fig. 10 (CA1: *Aii*; DG: *Bii*). As can be seen, the preferred phase angles for both theta (small ●) and the SO (small ○) for every experiment (except 1 SO example in the DG) was located in a cluster on the left half of the unit circle between  $90^\circ$  and  $270^\circ$  (i.e., on the falling phase of the ongoing field cycle). The distribution of these values was subjected to a second-order analysis (see METHODS section) and the average preferred angle across all experiments calculated (TH: large ●; SO: large ○). In every case, these averages were distributed close to  $180^\circ$  (CA1: TH  $167^\circ$ , SO  $160^\circ$ ; DG: TH  $166^\circ$ , SO  $191^\circ$ ). With the

exception of the SO in the DG, these distributions were all significantly different from homogeneity [CA1: TH  $f(2,2) = 44.26$ ,  $P < 0.05$ ; SO  $f(2,3) = 13.48$ ,  $P < 0.05$ ; DG: TH  $f(2,4) = 19.18$ ,  $P < 0.05$ ; SO  $f(2,4) = 2.92$ ,  $P > 0.05$ ].

An average distribution of normalized slope values across phase bins was also calculated across all experiments and is shown in the *right-most panels* of Fig. 10 (CA1: *Aiii*; DG: *Biii*). For illustrative purposes, a sine wave delineating the field cycle is superimposed on the data for theta (■) and SO (□). There is a clear cyclical modulation of slope values as a function of the ongoing phase of the field cycle for both TH and SO in both regions. These distributions were further subjected to a circular statistical analysis. The average preferred angle is denoted for both theta (▼) and SO (▽) for each of the distributions. Again, these values were located on the falling phase of the ongoing field cycle and were similar to those reported in the preceding text (CA1: TH  $167^\circ$ , SO  $153^\circ$ ; DG: TH  $165^\circ$ , SO  $181^\circ$ ).

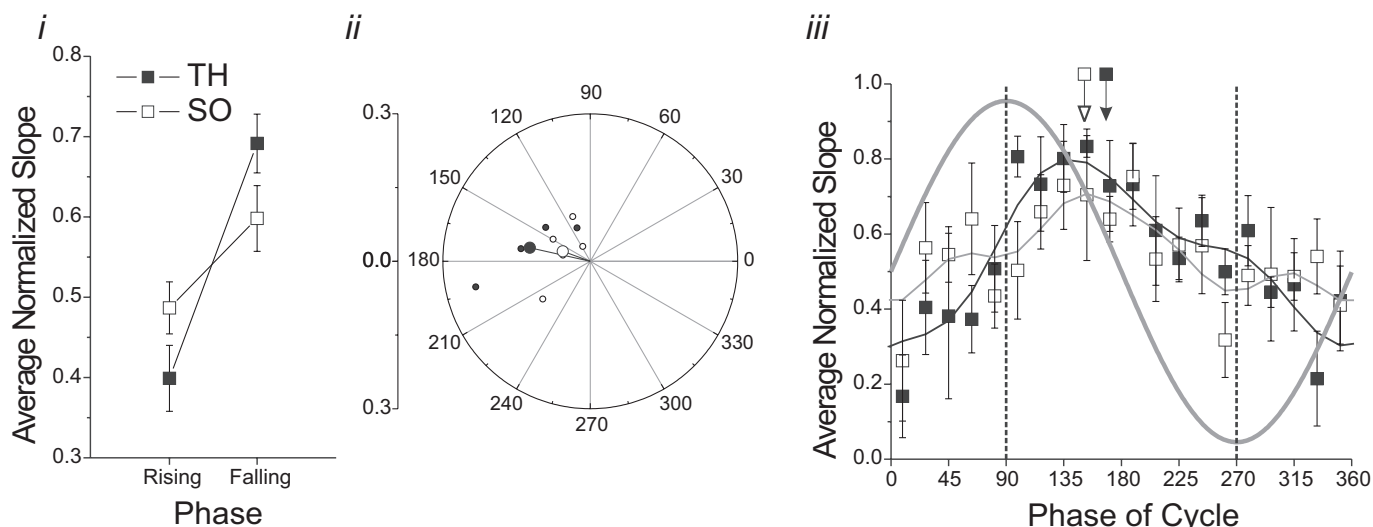
## DISCUSSION

Consistent with past research (Buzsáki et al. 1981; Fox 1989; Leung 1980; Segal 1978; Winson and Abzug 1978; Wyble et al. 2000), we have confirmed that spontaneous fluctuations in hippocampal electrographic state produced a significant modulation of synaptic excitability in a variety of hippocampal pathways. Importantly, three novel findings have emerged. 1) The direction of changes in synaptic excitability across states was specific for the particular pathway studied. Our data complement and extend those of previous researchers, who documented opposite changes with state when comparing PP stimulation with CA3 stimulation (Herreras et al. 1988; Winson and Abzug 1978) by further showing that stimulation of the two branches of the PP (medial and lateral) yielded independent and contrasting state-dependent effects. This demonstrates that electrographic state in the hippocampal network provides an even more complex modulation of inputs arriving to and being processed by the HPC than originally thought. 2) The recently described SO state (Wolansky et al. 2006) promoted changes in hippocampal excitability that distinguish it from both the theta and LIA states. Thus this provides further evidence that the SO is a separate and specific state of hippocampal activity. 3) Significant variations of excitability within the rhythmic state of SO (similar to our and others results for theta) were predicted by the ongoing phase of the field cycle. Altogether, these findings have important implications for the processing and storage of information by the HPC and may provide clues to the communication and potential consolidation strategies employed in the cortico-hippocampocortical circuit that are crucial for declarative memory processes.

### Significance of state-dependent fluctuations in hippocampal excitability

Hippocampal processing is well known to be important for mnemonic processes (Eichenbaum 2004; Squire 1992). Its memory-related functions are thought to be engaged not only during wakefulness, when learning occurs and behavioral performance is engaged, but also during the patterns of activity that occur during “resting” periods (e.g., sleep) subsequent to

## A CA3-CA1



## B PP-DG

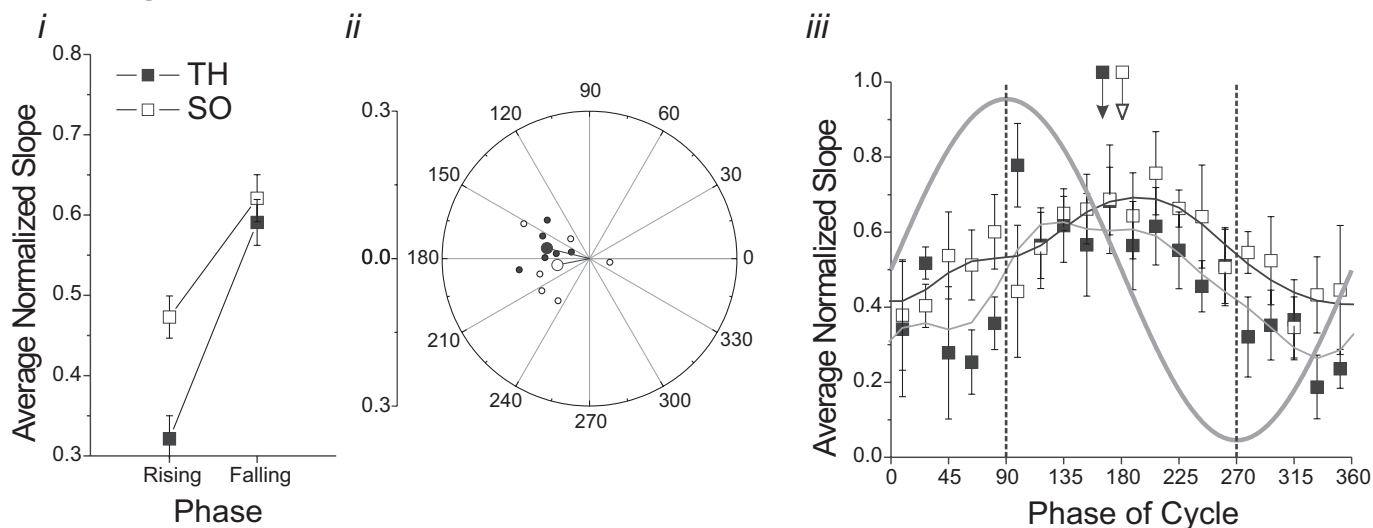


FIG. 10. Modulation of excitability across ongoing rhythmic cycles. Average normalized CA1 (A) and DG (B) pEPSP slope values after CA3 and PP stimulation, respectively, as a function of stimulation on differing oscillatory phases of theta or the SO. *i*: slope values were significantly higher during the rising phase as compared with the falling phase for both theta (■) and the slow oscillation (□) in CA1 (*Ai*) and DG (*Bi*) regions. *ii*: polar plots of the phase angle at which the maximal slope occurred for every experiment in the CA1 (*Aii*) and DG (*Bii*) region (theta: ●; slow oscillation: ○). In every case except 1, angles are clustered between 90 and 180°, which corresponds to the 1st half of the falling phase of the respective oscillation. Average vectors across all experiments are also plotted as larger-sized symbols and show a very tight distribution within the same quadrant. *iii*: slope values were averaged across all experiments as a function of discrete bins and plotted during theta (■) and the SO (□) for both the CA1 (*Aiii*) and DG (*Biii*) regions. The superimposed sinusoidal gray waveform represents the field cycle at the appropriate phase for comparison. The delineation between rising and falling elements of the cycle is shown by the vertical line at 90°, whereas the delineation between the falling and rising elements of the cycle is shown by the vertical line at 270°. Similar modulation is seen across both the theta and SO cycles and also in both CA1 and DG regions. The phase of maximum average synaptic excitability is noted by ▼ (theta) and ▽ (SO) arrowheads.

the learning process (Born et al. 2006; Walker and Stickgold 2004). It is these patterns (such as those differentially expressed during REM and non-REM stages of sleep) that are thought to contribute to the long-term consolidation of declarative memories (Buzsáki 1989; Marshall et al. 2006; Rasch et al. 2007).

Recently we have shown that the expression of state-dependent alternations of activity that are present during sleep can also occur spontaneously under urethan anesthesia and that the similarities between the two suggest that urethane is a good model system for sleep itself (Clement et al. 2006; Dickson et al. 2007a,b). Indeed, and more specifically for collective activity in the hippocampus, previous researchers have exploited urethan as a model for a number of different patterns of

hippocampal activity that are expressed during sleep including theta, gamma, and sharp-waves (Penttonen et al. 1998; Ylinen et al. 1995a,b). Indeed the theta state has a similar and overlapping bandwidth (3–6 Hz in urethan vs. 4–7 Hz in REM sleep) (Leung 1985; Vanderwolf et al. 1977), and the SO has an identical bandwidth (centered at 1 Hz) across urethan anesthesia and slow-wave sleep (Wolansky et al. 2006). As well, both states across urethan and sleep are affected in the same fashion by cholinergic agents: theta is promoted by muscarinic agonism, whereas the SO is promoted by muscarinic antagonism (Robinson et al. 1977; Wolansky et al. 2006).

Our present findings suggest that the spontaneously expressed and state-dependent patterns of activity observed in the

HPC differentially regulate excitability in hippocampal input and output pathways. For example, CA1 excitability was observed to be maximal during the SO in response to stimulation of either CA3 or TA. Given that the SO is a prominent component of deep stages of slow-wave sleep, this implies that the output of CA1 is preferentially biased during these stages. Furthermore, given the dynamic correlation of the SO across the HPC and nCTX (Wolansky et al. 2006), this would mean that the timing of hippocampal output could be systematically synchronized and/or desynchronized with that in the nCTX. The coupling and decoupling of hippocampal and cortical ensembles achieved in this manner would be highly relevant for the associative and activity-dependent processes of long-term potentiation (LTP) and long-term depression (LTD) and could thus constitute a platform for the process of declarative memory consolidation.

Interestingly, and in contrast to the results for CA1, input to the DG was differentially modulated by state depending on which branch of the PP was stimulated. MPP stimulation produced a maximal response during theta, whereas LPP stimulation produced a maximal response during the SO. Responses during LIA, although variable, were intermediate to those between theta and the SO. This variability might be attributable to the difficulty in separating the stimulation and recording sites for each of the branches of the PP because most experiments had overlapping activation of both branches. However, the significant difference between the theta and SO states suggests that input from the medial EC via the MPP is preferentially processed by the DG during REM sleep, whereas input from the LPP via the lateral EC is preferentially processed by the DG during slow-wave sleep. The relevance of this difference is less clear although previous work has demonstrated differences in the hodological (Witter et al. 2000), physiological (Abraham and McNaughton 1984; Alonso and Klink 1993; Dahl et al. 1990; McNaughton 1980; Tahvildari and Alonso 2005), pharmacological (Bramham et al. 1988; Dahl and Sarvey 1989), and behavioral (Ferbinteanu et al. 1999; Hargreaves et al. 2005) significance of these two pathways in addition to the medial and lateral regions of the EC that give rise to them. State-dependent segregation via preferential processing of these two inputs at the level of the DG may very well have implications for the functional separation of episodic versus semantic declarative memory processes (Eichenbaum 2004, 2006).

Although mentioned in the preceding text, another finding related to the differential excitability of hippocampal input pathways relates to the TA. Like the LPP, the TA showed preferential excitability during the SO, suggesting that the direct entorhinal-CA1 pathway from EC is preferentially excitable during slow-wave sleep. One ramification of this would be enhanced reverberatory communication between the HPC and the EC within the entorhino-hippocampal loop (ECIII – CA1 – ECV – ECIII). The functionality of this reverberatory loop has been demonstrated physiologically (Kloosterman et al. 2004), and the importance of the TA in hippocampal-dependent mnemonic function has been demonstrated (Brun et al. 2002; Remondes and Schuman 2004). Oscillatory and synchronized reverberations within this circuit might mediate the solidification of medial temporal lobe representations during slow wave sleep.

Although our study of hippocampal pathways was extensive, further study of state-dependent influences in the remaining elements of the trisynaptic pathway is required. In particular, the mossy fiber pathway (DG-CA3) and the hippocampocortical pathway (CA1 to subiculum and EC) may show important differences in regards to state-dependent modulation. Indeed previous work suggests that the deep layers of the EC may be preferentially responsive to slow patterned activity as opposed to theta (Yun et al. 2002).

State-dependent changes in excitability of hippocampal circuitry are not only important for an understanding of physiological functioning but may also be relevant for pathology—especially that concerning epilepsies deriving from the medial temporal lobe. It is well known that certain forms of epilepsy can be expressed more prevalently during sleep, especially during non-REM stages (Foldvary-Schaefer and Grigg-Damberger 2006). Our findings might also be relevant for the sleep-related preponderance of epileptiform events deriving from medial temporal lobe structures (Herman et al. 2001). The SO may effectively reduce the threshold for hypersynchronous discharges in the HPC and may also result in an increased ability to generalize through cortical output pathways via the entorhinal cortex and medial temporal lobe (Herman et al. 2001). Further research is necessary to examine this possibility.

#### *Cycle by cycle modulation of hippocampal excitability*

Not only was state an important modulator of synaptic responsiveness but within each rhythmic state, whether theta or the SO, so too was the phase of the oscillatory field cycle. Such modulation provides the HPC with an even more fine-grained temporal mechanism to influence processing. In both CA1 and DG regions, the slope of the EP was larger during the falling phase of the cycle than the rising phase and excitability was systematically modulated across phases. Although previous researchers have documented similar results for the theta rhythm (Buzsáki et al. 1981; Rudell and Fox 1984; Rudell et al. 1980; Wyble et al. 2000), this is the first demonstration of such a cyclical modulation for the SO in the HPC.

For both cycles, the falling phase of the extracellular field potential rhythm corresponds to a transition point where the net flow of current is moving out of the extracellular medium and entering the intracellular space. At the intracellular level, this corresponds very simply to a transition from a more hyperpolarized level to one that is more depolarized. Thus the timing of enhanced synaptic efficacy is set to the period at which the membranes of postsynaptic neurons are moving toward the just-subthreshold range. Synaptic input arriving at these moments are likely to bring the postsynaptic membrane to threshold and discharge the cell earlier in the cycle than would occur spontaneously. A similar mechanism that additively couples linearly increasing excitation with subthreshold oscillatory activity is proposed to underlie the phase precession shown by hippocampal place cells relative to the ongoing theta rhythm as the animal passes through its spatial receptive field (Harris et al. 2002; Mehta et al. 2002; O'Keefe and Recce 1993). Our results show that there may also be a further cyclic modulation of synaptic excitability with respect to the field oscillation that is also phase-locked to the ongoing oscillation. One effect that this might have would be to extend the effective phase range of precession that is possible within an oscillatory cycle. Al-

though it is unclear how phase precession occurring through phase-coupled enhancements in synaptic transmission might be important for processing during either hippocampal theta or SO within sleep, certainly the relative timing of discharge with respect to other neurons would have functional implications for ensemble binding and for plasticity (Holscher et al. 1997; Hyman et al. 2003; Pavlides et al. 1988).

#### ACKNOWLEDGMENTS

We thank T. Wolansky for technical help and C. Harley for insightful input regarding early findings.

#### GRANTS

This study was supported by Canadian Institutes of Health Research Grant MOP77625 to C. T. Dickson. C. T. Dickson is an Alberta Heritage Foundation for Medical Research Scholar.

#### REFERENCES

- Abraham WC, McNaughton N. Differences in synaptic transmission between medial and lateral components of the perforant path. *Brain Res* 303: 251–260, 1984.
- Alonso A, Klink R. Differential electroresponsiveness of stellate and pyramidal-like cells of medial entorhinal cortex layer II. *J Neurophysiol* 70: 128–143, 1993.
- Axmacher N, Mormann F, Fernandez G, Elger CE, Fell J. Memory formation by neuronal synchronization. *Brain Res Rev* 52: 170–182, 2006.
- Bland BH. The physiology and pharmacology of hippocampal formation theta rhythms. *Prog Neurobiol* 26: 1–54, 1986.
- Bodizs R, Bekesy M, Szucs A, Barsi P, Halasz P. Sleep-dependent hippocampal slow activity correlates with waking memory performance in humans. *Neurobiol Learn Mem* 78: 441–457, 2002.
- Born J, Rasch B, Gais S. Sleep to remember. *Neuroscientist* 12: 410–424, 2006.
- Bramham CR, Errington ML, Bliss TV. Naloxone blocks the induction of long-term potentiation in the lateral but not in the medial perforant pathway in the anesthetized rat. *Brain Res* 449: 352–356, 1988.
- Brun VH, Otnass MK, Molden S, Steffenach HA, Witter MP, Moser MB, Moser EI. Place cells and place recognition maintained by direct entorhinal-hippocampal circuitry. *Science* 296: 2243–2246, 2002.
- Buzsáki G. Hippocampal sharp waves: their origin and significance. *Brain Res* 398: 242–252, 1986.
- Buzsáki G. Two-stage model of memory trace formation: a role for “noisy” brain states. *Neurosci* 31: 551–570, 1989.
- Buzsáki G. Theta oscillations in the hippocampus. *Neuron* 33: 325–340, 2002.
- Buzsáki G, Grastyan E, Czopf J, Kellenyi L, Prohaska O. Changes in neuronal transmission in the rat hippocampus during behavior. *Brain Res* 225: 235–247, 1981.
- Canning KJ, Leung LS. Lateral entorhinal, perirhinal, and amygdala-entorhinal transition projections to hippocampal CA1 and dentate gyrus in the rat: a current source density study. *Hippocampus* 7: 643–655, 1997.
- Canning KJ, Wu K, Peloquin P, Kloosterman F, Leung LS. Physiology of the entorhinal and perirhinal projections to the hippocampus studied by current source density analysis. *Ann NY Acad Sci* 911: 55–72, 2000.
- Clement E, Thwaites M, Richard A, Ailon J, Peters S, Dickson C. Sleep-like rhythmic alternations of brain state under urethane anesthesia. *Soc Neurosci Abstr* 361.361, 2006.
- Dahl D, Burgard EC, Sarvey JM. NMDA receptor antagonists reduce medial, but not lateral, perforant path-evoked EPSPs in dentate gyrus of rat hippocampal slice. *Exp Brain Res* 83: 172–177, 1990.
- Dahl D, Sarvey JM. Norepinephrine induces pathway-specific long-lasting potentiation and depression in the hippocampal dentate gyrus. *Proc Natl Acad Sci USA* 86: 4776–4780, 1989.
- Dickson C, Lo A, Clement E, Richard A. Cyclical and sleep-like alternations of brain state under urethane anaesthesia. *Can J Neurol Sci* 3, Suppl S5: 9B109 2007a.
- Dickson C, Lo A, Clement E, Mah E, Richard A. Cyclical and sleep-like alternations of brain state are specific to urethane anaesthesia. *Soc Neurosci Abstr* 791.793, 2007b.
- Eichenbaum H. Hippocampus: cognitive processes and neural representations that underlie declarative memory. *Neuron* 44: 109–120, 2004.
- Eichenbaum H. Remembering: functional organization of the declarative memory system. *Curr Biol* 16: R643–645, 2006.
- Ferbinteanu J, Holsinger RM, McDonald RJ. Lesions of the medial or lateral perforant path have different effects on hippocampal contributions to place learning and on fear conditioning to context. *Behav Brain Res* 101: 65–84, 1999.
- Foldvary-Schaefer N, Grigg-Damberger M. Sleep and epilepsy: what we know, don't know, and need to know. *J Clin Neurophysiol* 23: 4–20, 2006.
- Fox SE. Membrane potential and impedance changes in hippocampal pyramidal cells during theta rhythm. *Exp Brain Res* 77: 283–294, 1989.
- Freeman WJ. *Mass Action in the Nervous System*. New York: Academic, 1975.
- Greenstein YJ, Pavlides C, Winson J. Long-term potentiation in the dentate gyrus is preferentially induced at theta rhythm periodicity. *Brain Res* 438: 331–334, 1988.
- Hahn TT, Sakmann B, Mehta MR. Phase-locking of hippocampal interneurons' membrane potential to neocortical up-down states. *Nat Neurosci* 9: 1359–1361, 2006.
- Hahn TT, Sakmann B, Mehta MR. Differential responses of hippocampal subfields to cortical up-down states. *Proc Natl Acad Sci USA* 104: 5169–5174, 2007.
- Hargreaves EL, Rao G, Lee I, Knierim JJ. Major dissociation between medial and lateral entorhinal input to dorsal hippocampus. *Science* 308: 1792–1794, 2005.
- Harris KD, Henze DA, Hirase H, Leinekugel X, Dragoi G, Czurko A, Buzsáki G. Spike train dynamics predicts theta-related phase precession in hippocampal pyramidal cells. *Nature* 417: 738–741, 2002.
- Herman ST, Walczak TS, Bazil CW. Distribution of partial seizures during the sleep-wake cycle: differences by seizure onset site. *Neurology* 56: 1453–1459, 2001.
- Herreras O, Solis JM, Munoz MD, Martin del Rio R, Lerma J. Sensory modulation of hippocampal transmission. I. Opposite effects on CA1 and dentate gyrus synapses. *Brain Res* 461: 290–302, 1988.
- Holscher C, Anwyl R, Rowan MJ. Stimulation on the positive phase of hippocampal theta rhythm induces long-term potentiation that can be depotentiated by stimulation on the negative phase in area CA1 in vivo. *J Neurosci* 17: 6470–6477, 1997.
- Hyman JM, Wyble BP, Goyal V, Rossi CA, Hasselmo ME. Stimulation in hippocampal region CA1 in behaving rats yields long-term potentiation when delivered to the peak of theta and long-term depression when delivered to the trough. *J Neurosci* 23: 11725–11731, 2003.
- Isomura Y, Sirota A, Ozen S, Montgomery S, Mizuseki K, Henze DA, Buzsáki G. Integration and segregation of activity in entorhinal-hippocampal subregions by neocortical slow oscillations. *Neuron* 52: 871–882, 2006.
- Jensen O, Lisman JE. Hippocampal sequence-encoding driven by a cortical multi-item working memory buffer. *Trends Neurosci* 28: 67–72, 2005.
- Ji D, Wilson MA. Coordinated memory replay in the visual cortex and hippocampus during sleep. *Nat Neurosci* 10: 100–107, 2007.
- Johnston D, Wu SM. *Foundations of Cellular Neurophysiology*. Cambridge, MA: MIT Press, 1995.
- Ketchum KL, Haberly LB. Synaptic events that generate fast oscillations in piriform cortex. *J Neurosci* 13: 3980–3985, 1993.
- Kloosterman F, van Haften T, Lopes da Silva FH. Two reentrant pathways in the hippocampal-entorhinal system. *Hippocampus* 14: 1026–1039, 2004.
- Leung LS. Behavior-dependent evoked potentials in the hippocampal CA1 region of the rat. I. Correlation with behavior and EEG. *Brain Res* 198: 95–117, 1980.
- Leung LS, Roth L, Canning KJ. Entorhinal inputs to hippocampal CA1 and dentate gyrus in the rat: a current-source-density study. *J Neurophysiol* 73: 2392–2403, 1995.
- Leung LW. Spectral analysis of hippocampal EEG in the freely moving rat: effects of centrally active drugs and relations to evoked potentials. *Electroencephalogr Clin Neurophysiol* 60: 65–77, 1985.
- Marshall L, Helgadottir H, Mollle M, Born J. Boosting slow oscillations during sleep potentiates memory. *Nature* 444: 610–613, 2006.
- McNaughton BL. Evidence for two physiologically distinct perforant pathways to the fascia dentata. *Brain Res* 199: 1–19, 1980.
- Mehta MR, Lee AK, Wilson MA. Role of experience and oscillations in transforming a rate code into a temporal code. *Nature* 417: 741–746, 2002.
- O'Keefe J, Recce ML. Phase relationship between hippocampal place units and the EEG theta rhythm. *Hippocampus* 3: 317–330, 1993.

- Pavlidis C, Greenstein Y, Grudman M, Winson J.** Long-term potentiation in the dentate gyrus is induced preferentially on the positive phase of theta-rhythm. *Brain Res* 439: 383–387, 1988.
- Penttonen M, Kamondi A, Acsady L, Buzsáki G.** Gamma frequency oscillation in the hippocampus of the rat: intracellular analysis in vivo. *Eur J Neurosci* 10: 718–728, 1998.
- Rasch B, Buchel C, Gais S, Born J.** Odor cues during slow-wave sleep prompt declarative memory consolidation. *Science* 315: 1426–1429, 2007.
- Remondes M, Schuman EM.** Role for a cortical input to hippocampal area CA1 in the consolidation of a long-term memory. *Nature* 431: 699–703, 2004.
- Robinson TE, Kramis RC, Vanderwolf CH.** Two types of cerebral activation during active sleep: relations to behavior. *Brain Res* 124: 544–549, 1977.
- Rodriguez R, Haberly LB.** Analysis of synaptic events in the opossum piriform cortex with improved current source-density techniques. *J Neurophysiol* 61: 702–718, 1989.
- Rudell AP, Fox SE.** Hippocampal excitability related to the phase of theta rhythm in urethanized rats. *Brain Res* 294: 350–353, 1984.
- Rudell AP, Fox SE, Ranck JB.** Hippocampal excitability phase-locked to the theta rhythm in walking rats. *Exp Neurol* 68: 87–96, 1980.
- Segal M.** A correlation between hippocampal responses to interhemispheric stimulation, hippocampal slow rhythmic activity and behaviour. *Electroencephalogr Clin Neurophysiol* 45: 409–411, 1978.
- Squire LR.** Memory and the hippocampus: a synthesis from findings with rats, monkeys, and humans. *Psychol Rev* 99: 195–231, 1992.
- Steriade M, Nunez A, Amzica F.** A novel slow (<1 Hz) oscillation of neocortical neurons in vivo: depolarizing and hyperpolarizing components. *J Neurosci* 13: 3252–3265, 1993.
- Suzuki SS, Smith GK.** Spontaneous EEG spikes in the normal hippocampus. I. Behavioral correlates, laminar profiles and bilateral synchrony. *Electroencephalogr Clin Neurophysiol* 67: 348–359, 1987.
- Tahvildari B, Alonso A.** Morphological and electrophysiological properties of lateral entorhinal cortex layers II and III principal neurons. *J Comp Neurol* 491: 123–140, 2005.
- Vanderwolf CH.** Hippocampal electrical activity and voluntary movement in the rat. *Electroencephalogr Clin Neurophysiol* 26: 407–418, 1969.
- Vanderwolf CH, Kramis R, Robinson TE.** Hippocampal electrical activity during waking behavior and sleep: analyses using centrally acting drugs. *Ciba Found Symp*: 199–226, 1977.
- Walker MP, Stickgold R.** Sleep-dependent learning and memory consolidation. *Neuron* 44: 121–133, 2004.
- Winson J, Abzug C.** Neuronal transmission through hippocampal pathways dependent on behavior. *J Neurophysiol* 41: 716–732, 1978.
- Witter MP, Wouterlood FG, Naber PA, Van Haeften T.** Anatomical organization of the parahippocampal-hippocampal network. *Ann NY Acad Sci* 911: 1–24, 2000.
- Wolansky T, Clement EA, Peters SR, Palczak MA, Dickson CT.** The hippocampal slow oscillation: A novel EEG state and its coordination with ongoing neocortical activity. *J Neurosci* 26: 6213–6229, 2006.
- Wyble BP, Linster C, Hasselmo ME.** Size of CA1-evoked synaptic potentials is related to theta rhythm phase in rat hippocampus. *J Neurophysiol* 83: 2138–2144, 2000.
- Ylinen A, Bragin A, Nadasdy Z, Jando G, Szabo I, Sik A, Buzsáki G.** Sharp wave-associated high-frequency oscillation (200 Hz) in the intact hippocampus: network and intracellular mechanisms. *J Neurosci* 15: 30–46, 1995a.
- Ylinen A, Soltesz I, Bragin A, Penttonen M, Sik A, Buzsáki G.** Intracellular correlates of hippocampal theta rhythm in identified pyramidal cells, granule cells, and basket cells. *Hippocampus* 5: 78–90, 1995b.
- Yun SH, Mook-Jung I, Jung MW.** Variation in effective stimulus patterns for induction of long-term potentiation across different layers of rat entorhinal cortex. *J Neurosci* 22: RC214, 2002.
- Zar JH.** *Biostatistical Analysis*. Upper Saddle River, NJ: Prentice Hall, 1999.